Quaternary Geochronology 79 (2024) 101489

Contents lists available at ScienceDirect

Quaternary Geochronology

journal homepage: www.elsevier.com/locate/quageo

Estimating extinction time using radiocarbon dates

Salvador Herrando-Pérez [a,*], Frédérik Saltré [b,1]

[a] School of Biological Sciences, The University of Adelaide, Adelaide, South Australia, 5000, Australia
[b] Global Ecology Partuyarta Ngadluku Wardli Kuu, College of Science and Engineering, ARC Centre of Excellence for Australian Biodiversity and Heritage, GPO Box 2100, Flinders University, Adelaide, South Australia, 5001, Australia

ARTICLE INFO

Keywords:
Calibration
Fossil
Megafauna
Signor-lipps effect
Time series

ABSTRACT

The extinction of a species is a key demographic event often signalling major climatic, ecological and/or evolutionary shifts that can be investigated using the fossil record. In that context, radiocarbon (^{14}C) dating has become a popular tool to time and test for scenarios of extinction that can inform on how species respond to past and future ecosystem changes. We develop CRIWM, a method for estimating extinction (and arrival) time from time series of ^{14}C dates while accounting for probability density functions (PDF) deriving from ^{14}C calibration. The sister method GRIWM assumes normal chronometric errors and is inappropriate for ^{14}C chronologies as PDFs are often non-Gaussian and multi-modal. Compared to GRIWM, CRIWM reduces by 4-fold the gap between true and estimated extinction times and the width of the confidence intervals, and is less sensitive to sample size, dating errors and the temporal distribution of specimens in a species' fossil record. We build the *R* package *Rextinct* with three user-friendly functions for computing CRIWM and GRIWM, and the PDF moments, modes and intercepts of ^{14}C calibrations. CRIWM and GRIWM accept time series comprising only ^{14}C dates or observations (fossils, sightings) dated by multiple chronometric methods, and calibration curves for fossils sampled in the Northern and Southern Hemispheres and marine environments. For both methods, we implement two different estimators of extinction time whether they are reliant on a *p*-value (original conceptualization) or not (novel). CRIWM and *Rextinct* are robust tools to time extinction and arrival events using ^{14}C chronologies spanning the entire Holocene to 50,000 calendar years Before Present, and can be used to investigate demographic phenomena queried through the fossil record such as migrations, domestications and extirpations.

1. Introduction

Species extinctions are one of the main drivers and consequences of the evolution of life on Earth (Raup, 1994). Understanding these phenomena relies on building accurate timelines of species extinctions that are correlated with environmental disruptions like climate change or human activity. This approach is based primarily on dated fossil records (Dietl and Flessa, 2011; Mitchell and Rawlence, 2021; Swift et al., 2019) and has been heightened by the radiocarbon (^{14}C) dating of biological events (Marra, 2019; Taylor and Bar-Yosef, 2016) spanning the last 50,000 years – the current limits of ^{14}C dating (van der Plicht and Palstra, 2016). The popularity of ^{14}C dating rests on outstanding methodological developments (Hajdas et al., 2021), namely small, low-energy accelerator mass spectrometers (García-León, 2018), improved laboratory protocols of collagen purification of fossilized skeletal materials (Herrando-Pérez, 2021), regularly updated calibration curves integrating multiple palaeo-archives (Heaton et al., 2020a), and sophisticated statistical approaches to analyze ^{14}C chronologies (Crema and Bevan, 2021).

Estimates of extinction time from the fossil record require statistical *post-hoc* corrections to account for the 'Signor-Lipps' effect (Raup, 1986) whereby the youngest of a series of dated observations is unlikely to belong to the last surviving individual of an extinct population or species (Signor and Lipps, 1982). A family of 'frequentist' statistical techniques (see Rivadeneira et al., 2009) has been developed to estimate species extinction time from sighting rates of living individuals (Boakes et al., 2015) or from time series of dated fossils (Wang and Marshall, 2016). However, even recent techniques, such as the Gaussian-Resampled Inverse-Weighted McInerny Method (GRIWM, Bradshaw et al., 2012), assume that the inherent errors (mathematically expressed as a confidence interval) in each date of a time series are normally distributed (Bradshaw et al., 2012; Saltré et al., 2015; Solow et al., 2006). This

* Corresponding author.
E-mail address: salherra@gmail.com (S. Herrando-Pérez).
[1] (EpicAustralia.org).

https://doi.org/10.1016/j.quageo.2023.101489
Received 6 April 2023; Received in revised form 21 October 2023; Accepted 2 November 2023
Available online 9 November 2023

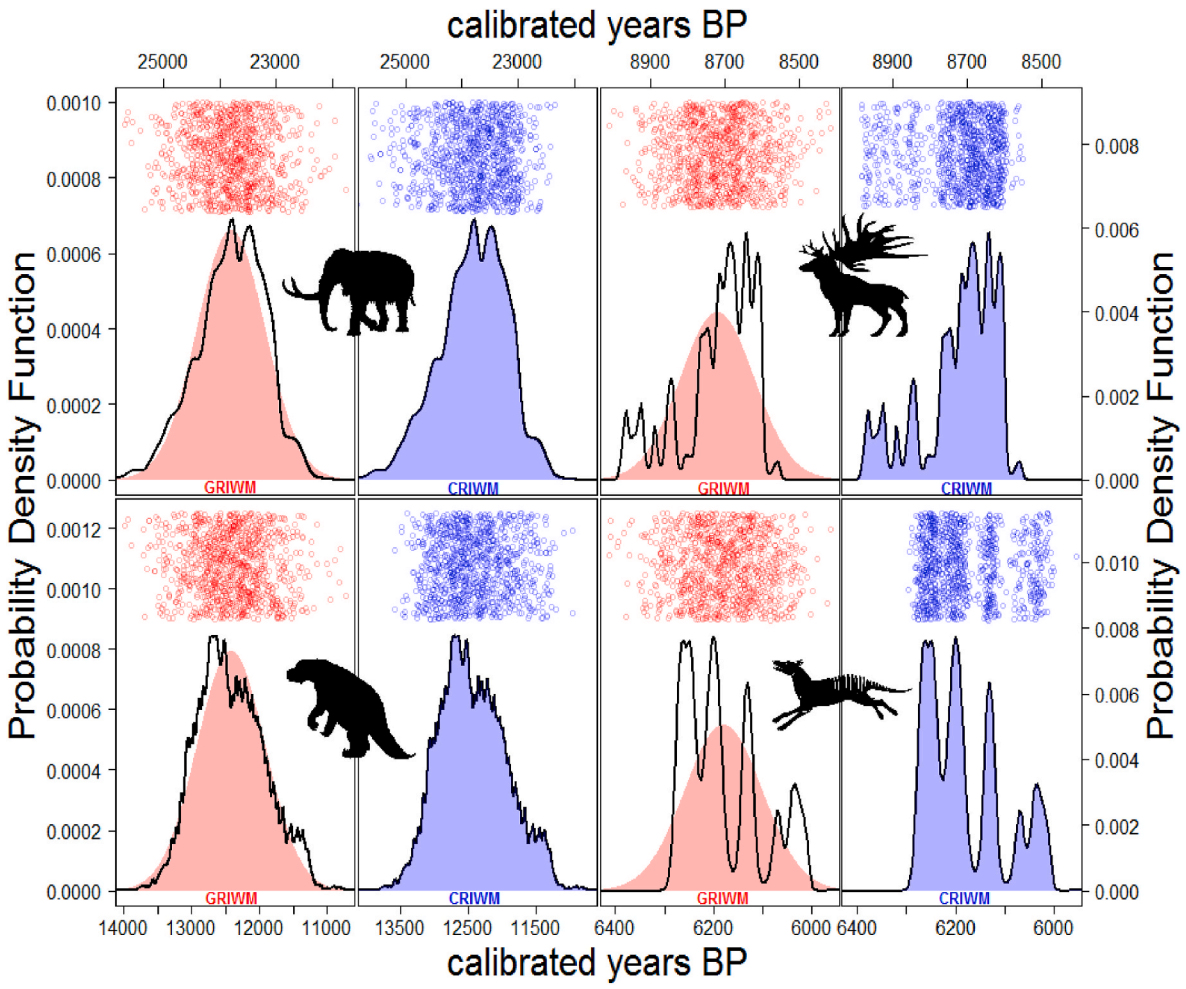

Fig. 1. Probability Density Function (PDF = bold line, y-axis) of four radiocarbon (^{14}C) dates of skeletal remains of megafauna species* in calendar years Before Present (BP) (x-axis). In the context of estimating extinction time from time series of ^{14}C dates, coloured surfaces indicate the probability surface used by GRIWM (red) and CRIWM (blue) to re-sample 1000 values (points) taken randomly from each PDF. ^{14}C dates calibrated with the *IntCal20* (mammoth, deer/Northern Hemisphere) and *SHCal20* (sloth, thylacine/Southern Hemisphere) calibration curves. The higher the probability, the more likely that a calibrated value will be re-sampled. ^{14}C dates (calibrated weighted average ± 1SD in calendar years): OxA-10122 = 23,727 ± 605 (ultrafiltered collagen, tooth of woolly mammoth *Mammuthus primigenius*, Cueto de la Mina/Asturias, Spain) (Stuart et al., 2002), OxA-23412 = 8712 ± 91 (ultrafiltered collagen, maxilla of giant deer *Megaloceros giganteus*, Preobrazhenka/Novosibirsk, Russia) (Lister and Stuart, 2019), CAMS-171861 = 12,349 ± 496 (XAD-purified collagen, metacarpal of giant ground sloth *Megatherium americanum*, Campo Laborde/Unión, Argentina) (Politis et al., 2019), ANU-43738 = 6174 ± 75 (ultrafiltered collagen, tibia of thylacine *Thylacinus cynocephalus*, Mundrabilla, Western Australia) (White et al., 2018).

assumption has yet to be tested for ^{14}C dates because the distributional properties of ^{14}C errors result from a Probability Density Function (PDF) calculated from ^{14}C calibrations and often fail to follow a Gaussian distribution (Telford et al., 2004). Due to the former assumption, authors studying the timing of extinction have neglected frequentist techniques for ^{14}C chronologies (Holdaway et al., 2014).

Here we introduce the Calibration-Resampled Inverse-Weighted McInerny Method (CRIWM), a modified version of GRIWM adapted to account for the true PDF resulting from ^{14}C calibrations and eliminates the assumption of normality of dating errors. We also build the *R* package *Rextinct* to compute CRIWM, GRIWM and calibrate ^{14}C dates in calendar years. Our study highlights the importance of integrating age uncertainty to analyse time series of dated observations (Boakes et al., 2015) for the particular case of ^{14}C chronologies.

2. Methods

Firstly, we present the three mathematical properties shared by CRIWM and GRIWM. Secondly, we present the mathematical properties that distinguish CRIWM. Thirdly, we provide two new developments equally applicable to CRIWM and GRIWM. Forthly, we describe a sensitivity analysis comparing the accuracy and precision of CRIWM *versus* GRIWM. Finally, we present the functionality of a new *R* package (*Rextinct*) to implement CRIWM and GRIWM in Appendix A, and expand our methods and results in the online Supplementary Material (sections SM1 to SM7).

2.1. GRIWM's original properties shared by CRIWM

1. Probability of extinction: CRIWM and GRIWM correct for the assumption that the probability of sighting rates or fossil frequencies follows a uniform distribution (Saltré et al., 2015), which is also assumed to be indicative of population abundance (McInerny et al., 2006). Both methods define extinction time as the year (t_0) at which the probability (P) of finding a new fossil or living individual at a date younger than the youngest known observation has a target value $P = \alpha$ (defined *a priori* by the investigator) following:

$$\widehat{t_\theta} = t_n - \frac{\log \alpha}{\log\left(1 - \frac{n}{t_n - t_0}\right)} \quad (1)$$

where, for $n+1$ dated records in chronological order $t_0 < t_1 < \ldots < t_n < t_\theta$, the probability to detect no fossil between the last fossil date t_n and a previous date A is $P = (1-p)^{A-t_n}$ with p being the probability to detect a fossil in a given year. This probability p is estimated based on the sighting rate ($\frac{n}{t_0 - t_n}$). CRIWM and GRIWM produce an estimate $\widehat{t}$ of the upper bound (95%) of the $P = \alpha$ confidence interval ($\alpha = 0.05$) of t_0 (Bradshaw et al., 2012; McInerny et al., 2006).

2. Down-weighting of temporal gaps: Unlike McInerny et al. (2006), CRIWM and GRIWM account for the fact that t_θ is highly sensitive to n (Rivadeneira et al., 2009; Saltré et al., 2015; Solow, 2005). Thus, Bradshaw et al. (2012) argued that observations closer to t_θ should contribute quantitatively more to the estimate of the extinction time t_θ so that its final estimator $\widehat{t_{\theta_F}}$ is:

$$\widehat{t_{\theta_F}} = \frac{\sum_{k=1}^{n} \omega_k \widehat{t_{\theta_k}}}{\sum_{k=1}^{n} \omega_k} \quad (2)$$

where $\widehat{t_{\theta k}}$ is the intermediate iterative estimate for all possible time series lengths (from $k = 2$ to $k = n$) associated with each time series length's relative weight contribution $\omega_k = \frac{1}{t_n - t_k}$.

3. Re-sampling of dating errors: Before applying CRIWM and GRIWM to a time series of ^{14}C dates, each date (age ± 1 standard deviation in years as provided by a ^{14}C dating facility) must be converted to calendar years using a calibration curve and resolves into a unique PDF (Keenan, 2012). This step was removed in the original description of GRIWM because all dates in a time series were assumed to be in calendar years whether they had been obtained by ^{14}C dating and/or other chronometric methods. Further background about ^{14}C dating and calibrations is presented in Supplementary Material (SM1).

2.2. Properties distinguishing CRIWM from GRIWM

To account for the error associated with each calibrated date in a time series, GRIWM generates 10,000 times series, each resulting from re-sampling with replacement one value from the theoretically normal distribution of the error of each date (Saltré et al., 2015). Since GRIWM assumes that all calibrated dates in a time series have a normal PDF, the closer a value is to the PDF mean of any given date, the more likely this value will be re-sampled (Fig. 1). The extinction time $\widehat{t_{\theta_\omega}}$ (formula 2) is then calculated for each of the 10,000 re-sampled time series, hence resulting in 10,000 values of $\widehat{t_{\theta_\omega}}$. Ultimately, the final extinction time ($\widehat{t_{\theta_F}}$) and its confidence interval are calculated as the median with 95% inter-quantile ranges across the 10,000 $\widehat{t_{\theta_\omega}}$ (Saltré et al., 2015).

However, the shape of the PDF of a ^{14}C date varies considerably as a function of the width of the ^{14}C error resulting from the dating process (reviewed by Olsson, 1989), the non-linear production of ^{14}C in the atmosphere and the variability intrinsic to the carbon cycle (Hughen et al., 2004; Pavón-Carrasco et al., 2018; Roth and Joos, 2013). To illustrate this point numerically, we used 50,000 ^{14}C-simulated dated fossils (from 1 to 50,000 years BP with a 1 year increment) with a constant ^{14}C error of 50 years (see Supplementary Materials SM2 and SM3 for analyses of PDF normality and multimodality, respectively), and show that (*i*) 86–91 % of the PDFs of the *IntCal20*-calibrated dates had a probability $p < 0.01$ if the null hypothesis of PDF normality was true for three normality tests (median $p <$ 9.4E-10; Tables S1 and S2; Fig. S1), and (*ii*) 3 of every 10 PDFs had 2 to 8 statistically supported modes (Tables S3 and S4). PDF multimodality was particularly strong between 1 and ~10,000 years BP (mostly falling in the Holocene epoch) with 8–9 of every 10 PDFs showing >2 modes (Fig. S3, Table S4). These results prevailed across constant ^{14}C errors from 125 to 1000 years (with PDFs showing up to 10 modes) and the *IntCal20* and *SHCal20* calibration curves (Figs. S1–S3, Tables S1–S4). Overall, our analysis clearly demonstrates that the PDFs of calibrated ^{14}C dates have extremely weak normality properties.

To relax GRIWM's stringent assumption of normally distributed errors, the new method CRIWM assumes that all ^{14}C dates in a study time series are non-calibrated in years, and the extinction time $\widehat{t_{\theta_F}}$ is obtained by generating 10,000 times series, each resulting from re-sampling with replacement of one value from the true PDF of each calibrated ^{14}C date. Therefore, for any given calibrated ^{14}C date (whatever its PDF shape), the closer a value is to one of the modes of the PDF, and the higher that mode is, the more likely that CRIWM will re-sample that value (Fig. 1). Like GRIWM, CRIWM's $\widehat{t_{\theta_F}}$ is the median with 95% inter-quantile ranges across the 10,000 $\widehat{t_{\theta_\omega}}$

2.3. Novel properties shared by CRIWM and GRIWM

1. Unbiased estimator: CRIWM and GRIWM rely on the time at which the extinction probability P reaches the target value $\alpha = 0.05$ returning the upper-bound (95%) estimator of the extinction time $\widehat{t_{\theta_F}}$. Since this implies that $\widehat{t_{\theta_F}}$ is a statistically biased estimators of t_θ (Frey, 2018; Lindgren, 2017), we also present here the unbiased version $\widehat{t_{\theta_u}}$ of this estimator (i.e., not relying on any target value α, see mathematical derivation in Supplementary Material SM4):

$$\widehat{t_{\theta_u}} = t_n \frac{n+1}{n} - \frac{t_0}{n} \quad (3)$$

where $\widehat{t_{\theta_u}}$ is the minimum theoretical date in a uniform distribution with n observations dated between t_n and t_0 (Solow 2005) and does not rely on p-values. The down-weighting and re-sampling steps in the biased and unbiased estimators of extinction time are identical, the two estimators only differing in the formulation of extinction time ($\widehat{t}$ in formula 1 *versus* $\widehat{t_{\theta_u}}$ in formula 3).

2. Arrival time: CRIWM and GRIWM can be used to estimate extinction time but also arrival time (see GRIWM examples in Douglass et al., 2019; Feranec and Kozlowski, 2016; Perez et al., 2016; Saltré et al., 2016). The statistical interpretation of the biased estimator for the arrival time in CRIWM or GRIWM follows a similar logic to that of extinction time (Bradshaw et al., 2012; Saltré et al., 2016) so that the arrival time equals (*biased estimator*) the year $\widehat{t_{\theta_F}}$ at which the probability of finding a new fossil or living individual dated older than the oldest known observation is 0.05 (formulas 1 and 2), or (*unbiased estimator*) the maximum theoretical year $\widehat{t_{\theta_u}}$ in a uniform distribution with n observations dated between t_n and t_0 (formula 3).

2.4. Sensitivity analysis

To examine the robustness of CRIWM and GRIWM, we run a sensitivity analysis in three stages: (*i*) simulating times series of ^{14}C dates for different sample sizes and time periods, (*ii*) comparing accuracy and precision of estimating extinction time by both methods, and (*iii*) evaluating the sensitivity of such accuracy and precision to the statistical properties of the simulated time series. We refer to 'time series' as a set of specimens from an extinct species whose ages have been determined by ^{14}C dating. For each time series, 'inaccuracy' (Δ) is the difference between the simulated true extinction time t_s and CRIWM's (or GRIWM's) estimate of extinction time $\widehat{t_{\theta_F}}$ or $\widehat{t_{\theta_u}}$ (the lower the difference, the higher the accuracy, the further away $\widehat{t_{\theta_F}}$ or $\widehat{t_{\theta_u}}$ are from t_s), and 'imprecision' (λ) is the width of the confidence interval of $\widehat{t_{\theta_F}}$ or $\widehat{t_{\theta_u}}$ (the narrower the confidence interval, the higher the precision).

Time series were simulated within a 'target interval' from 1 to

Table 1
Input parameters in the sensitivity analysis comparing the accuracy and precision of CRIWM *versus* GRIWM across 1000 simulated time series, where i = interval between two ^{14}C dates (years) and ε = error of each ^{14}C date (years). Each time series fell within a target interval from 1 to 14,706 years Before Present (BP), and resulted in one true extinction date (t_s) and four sister estimates of extinction time by CRIWM *versus* GRIWM using biased ($\widehat{t_{\theta_E}}$) *versus* unbiased ($\widehat{t_{\theta_u}}$) estimators (Figs. 3 and 4).

Name	Description	Metrics from simulated time series
n	number of ^{14}C dates	[3, 100]
t_s	simulated true extinction date	[206.0, 11.2 × 10^3] years BP
$\bar{i}$	average i over the entire time series	[1.1, 2.9 × 10^3] years
σ_i^2	variance of i over the entire time series	[0.2, 8.4 × 10^6] years^2
$\bar{\varepsilon}$	average ε over the entire time series	[59.9, 4.1 × 10^3] years
σ_ε^2	variance of ε over the entire time series	[2.1 × 10^3, 9.2 × 10^6] years^2

14,706 non-calibrated years BP – defined as the finite range of ^{14}C dates in which the PDFs resulting from ^{14}C calibrations maximize their multimodality through the *IntCal20* and *SHCal20* calibration curves (target interval calculated in Supplementary Material SM3, Table S5). Such interval should enhance the comparison of CRIWM *versus* GRIWM performance because their main statistical difference is that re-sampling assumes a unimodal PDF for each ^{14}C date in a time series in GRIWM but their true (unimodal to multimodal) PDF in CRIWM (Fig. 1). Additionally, the target interval encompasses a period rich in species extinctions (Elias, 2023), like those of mammoths in Eurasia and North America (Nogués-Bravo et al., 2008) and most megafauna from large islands (Kouvari and van der Geer, 2018), and human migrations such as the peopling of the Pacific (Pugach et al., 2021). Previous examinations of GRIWM's performance did not justify their target interval (15,000 to 20,000 and 10,000 to 15,000 calibrated years BP in Bradshaw et al. (2012) and Saltré et al. (2015), respectively) as they did not attempt to control for PDF shape along the ^{14}C calibration curve.

Each simulated time series covered a different period, with ^{14}C dates being randomly sampled from the target interval [1, 14,706] years BP, and was generated by randomly varying four parameters: (1) the extinction time (t_s), (2) the number of dates (n), (3) the type of ^{14}C error associated with each ^{14}C date whether random or proportionally increasing as ^{14}C dates get older in a fossil record, and (4) the underlying probability distribution of specimens being deposited, fossilized and recovered whether uniform, exponential, sigmoidal or logarithmic (after Bradshaw et al., 2012) — the formulation of those four distributions is presented in Supplementary Material SM5 (Table S6). We generated 1000 simulated time series by stochastically selecting single values of the parameter quadruplet (Table 1) covering the full parameter space under a *Latin hypercube* sampling approach (McKay et al., 1979; Saltelli et al., 2007). Such sampling ensures that all parameters are represented in a fully stratified design, without prior knowledge of their influence on CRIWM and GRIWM outputs.

We applied CRIWM's and GRIWM's biased and unbiased estimators to the 1000 simulated time series (Table 1), so totalling four computation runs (2 methods × 2 estimators) per response (Δ or λ) resulting in four sets of estimates of extinction time per time series. Δ and λ and the sensitivity analysis were computed for each CRIWM and GRIWM run. We used the Hilbert-Schmidt Independence Criterion (HSIC, Gretton et al., 2005) to quantify the relative effect (*sensitivity*) of five factors on Δ

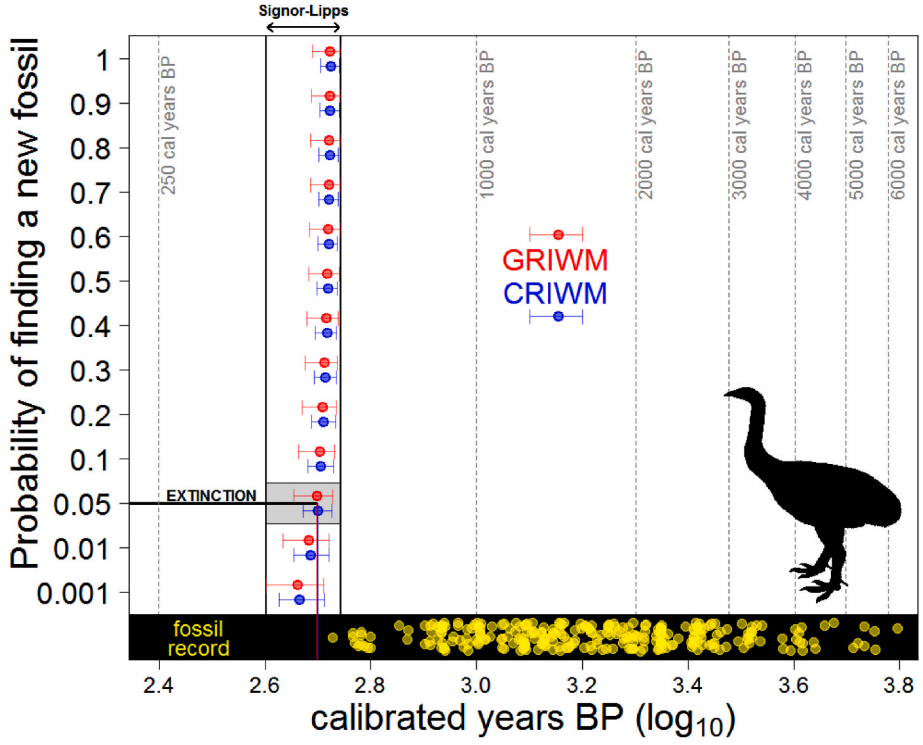

Fig. 2. Conceptualization of the Signor-Lipps effect using a time series of 270 radiocarbon (^{14}C) dates (yellow circles) of moa in the South Island of New Zealand. CRIWM and GRIWM estimate extinction time (biased estimator $\widehat{t_{\theta_E}}$) as the calendar year (x-axis) at which the probability of finding a specimen younger than the youngest known specimen is 0.05 (y-axis). For each date in calendar years, GRIWM assumes a normal error while CRIWM accounts for the true probability density function of such error. Probabilities shown as medians (dots) with 95% inter-quantile ranges (bars) for GRIWM (red) and CRIWM (blue) over 10,000 re-sampled time series. Extinction time (Probability = 0.05) estimated at 500 [532, 470] and 497 [539, 446] calendar years Before Present (BP) by CRIWM and GRIWM, respectively (Table S7). The Signor-Lipps effect captures the uncertainty that the last fossil of an extinct species is unlikely to belong to the last surviving individual. Data obtained from Holdaway et al. (2014) for 268 bones and two coprolites from bush moa *Anomalopteryx didiformis*, South Island giant moa *Dinornis robustus*, Eastern moa *Emeus crassus*, broad-billed moa *Euryapteryx curtus*, upland moa *Megalapteryx didinus*, crested moa *Pachyornis australis* and heavy-footed moa *Pachyornis elephantopus*. All ^{14}C dates calibrated with *SHCal20*.

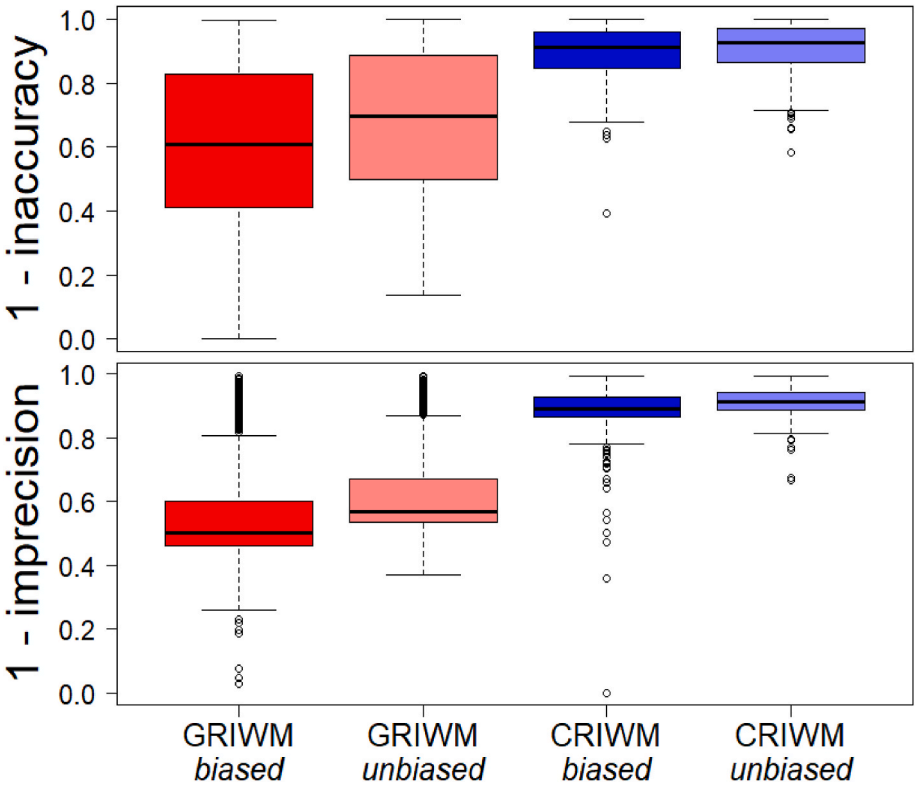

Fig. 3. Inaccuracy and imprecision of the biased and biased estimators of extinction time obtained by CRIWM and GRIWM on each of 1000 simulated time series each representing an extinct species with 3–100 specimens dated by ^{14}C dating (input parameters summarized in Table 1). Inaccuracy is the difference between the simulated true extinction time (t_s) and the estimated extinction time (the lower the difference, the higher the accuracy) and imprecision is the width of the confidence interval (the narrower the confidence interval, the higher the precision) — both metrics in calendar years. Values standardized to a reverse (1 – inaccuracy = accuracy, 1 – imprecision = precision) binary ([0,1]) scale by the maximum inaccuracy and imprecision across the 1000 time series collectively obtained by $GRIWM_{biased}$, $GRIWM_{unbiased}$, $CRIWM_{biased}$ and $CRIWM_{unbiased}$, such that the accuracy and precision of the estimated extinction times across time series increase from 0 to 1.

or λ following Saltré et al. (2015): (1) the number of dated fossils (n), (2) the average ($\bar{i}$) and (3) variance (σ_i^2) of the time step between pairs of consecutive ^{14}C dates, and (4) the average ($\bar{\varepsilon}$) and (5) variance (σ_ε^2) of the dating errors across all ^{14}C dates in a time series (Table 1). A form of kernel-based regression, HSIC accounts for non-linear and non-monotonic effects and collinearity among predictors and handles distribution-free residuals (Da Veiga, 2015; Gretton et al., 2005). The HSIC of each predictor was expressed as the median and 95% inter-quantile range of 1000 bootstrapped replicates using the *R* function *sensitivity::sensiHSIC* (Iooss et al., 2021).

3. Results

3.1. Extinction time of moas

We applied CRIWM and GRIWM to moa ^{14}C dates spanning 564 to 5503 ^{14}C years BP obtained from 270 specimens collected on the South Island of New Zealand (Holdaway et al., 2014). These authors combined the timing of moa extinction and exploitation of moa eggs with human population growth to argue that Polynesians drove moa to extinction through hunting and habitat modification. Our estimate of moa extinction ($P = 0.05$, formula 1) with *SHCal13* was 501 [533, 471] for CRIWM and 499 [535, 451] calendar years for GRIWM (Table S7), therefore only ~2 decades younger, and importantly with a confidence interval (CRIWM) 22 years narrower, than a previous Bayesian estimate of extinction at 524 with a 95% credible interval of [554, 470] calendar years BP (Holdaway et al., 2014). We report CRIWM and GRIWM extinction times (formula 2) at 13 different probabilities from $P = 0.001$ to $P = 1$ (formula 2) for *SHCal20* in Fig. 2, and for *SHCal13* and *SHCal20* in Table S7 (Supplementary Material SM6).

3.2. Accuracy and precision (estimates and sensitivities)

Across the 1000 simulated time series, CRIWM was four times more accurate (lower Δ) and precise (lower λ) than GRIWM, and the unbiased estimators were marginally more accurate and precise than the biased estimators (Fig. 3). Thus, the median Δ [±95% inter-quantile ranges] in years was $GRIWM_{biased}$ = 6314 [273–9552], $GRIWM_{unbiased}$ = 4812 [1518–8132], $CRIWM_{biased}$ = 1216 [341–2422], $CRIWM_{unbiased}$ = 563 [270–1818]. The median λ [±95% inter-quantile ranges] in years was $GRIWM_{biased}$ = 23,958 [19,063–25,770], $GRIWM_{unbiased}$ = 20,788 [15,688–22,313], $CRIWM_{biased}$ = 5162 [3399–6416], and $CRIWM_{unbiased}$ = 4209 [2695–5370].

CRIWM's Δ and λ were >50 and >30 % (respectively) less sensitive (i.e., less variable) than GRIWM's to variation in all predictors over the 1000 simulated time series (Fig. 4). Here, sensitivities were measured through HSIC (see Methods), so the higher the HSIC for a given predictor, the higher the sensitivity of Δ or λ (obtained by CRIWM or GRIWM) to variation in the magnitude of that predictor. Remarkably, HSIC for CRIWM's Δ neared 0 for n, σ_i^2 and σ_ε^2, denoting outstanding robustness to sample size and variability in fossil frequency and ^{14}C errors in a fossil record. Both methods' λ was most sensitive to the magnitude and variation of the ^{14}C errors in a time series as can be expected from estimations of extinction time that rely on 10,000-fold resampling of those errors. CRIWM's unbiased estimator marginally reduced the sensitivity of λ to all predictors, particularly n (Fig. 4).

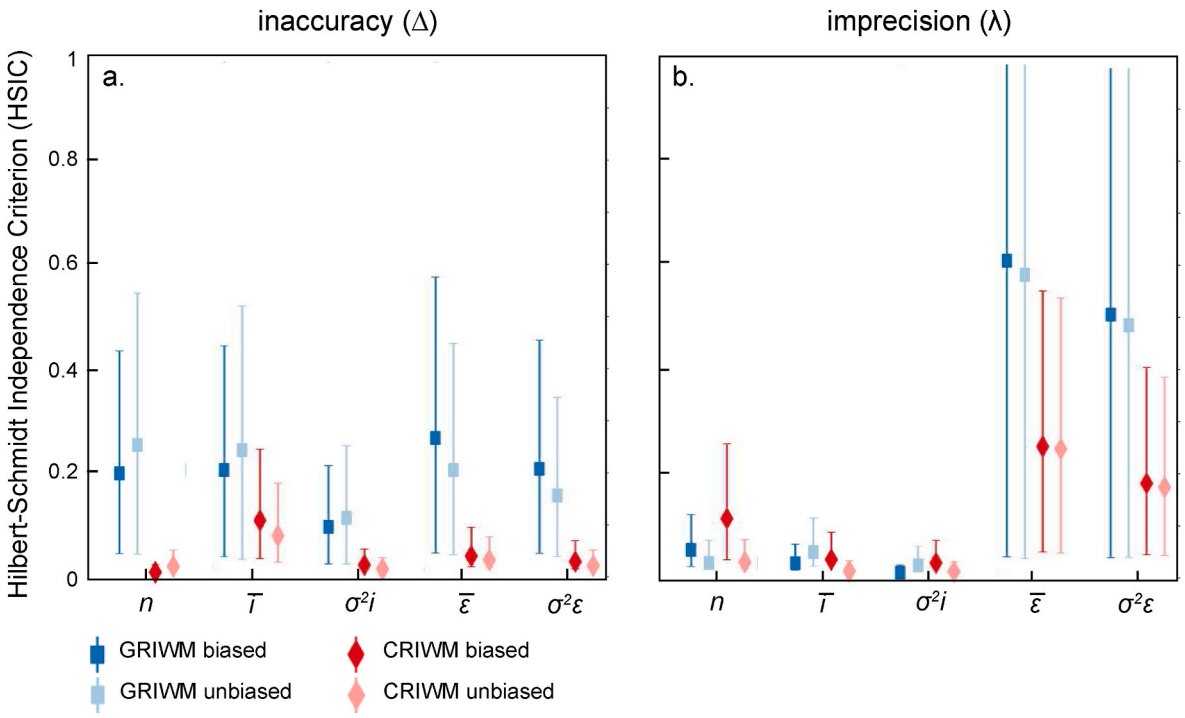

Fig. 4. Sensitivity to five predictors of the inaccuracy (Δ) and imprecision (λ) (responses in calendar years) of the biased ($\widehat{t_{0_F}}$) and biased estimators ($\widehat{t_{0_u}}$) of extinction time obtained by CRIWM and GRIWM on each of 1000 simulated time series each representing an extinct species with 3–100 specimens dated by ^{14}C dating. Δ is the difference between the true extinction time and the estimated extinction time (the lower the difference, the higher the accuracy) and λ is the width of the confidence interval (the narrower the confidence interval, the higher the precision). The predictors (summarized in Table 1) are the number of dated specimens (n), the average ($\bar{\imath}$, years) and variance (σ_i^2, years) of time step between pairs of consecutive dates, and the average ($\bar{\varepsilon}$, years) and variance (σ_ε^2, years) of ^{14}C dating error across dates. Sensitivity measured using the Hilbert-Schmidt Independent Criterion (HSIC, bootstrapped median ± 95% inter-quantile ranges), a kernel-based, non-parametric regression that captures the magnitude of variation in (separately) inaccuracy and imprecision caused by the variation of the predictors across all time series. The lower the HSIC, the lower the sensitivity for a response to a predictor.

4. Discussion

We have developed (1) the first frequentist method (CRIWM) that accounts for the true probability space resulting from ^{14}C calibrations to estimate extinction and arrival time from time series of ^{14}C dates, (2) two alternative estimators of extinction and arrival time whether they are reliant on *p*-values (biased) or not (unbiased), and (3) the first implementation of GRIWM and CRIWM in an *R* package (*Rextinct*). The weighting procedure of the GRIWM algorithm has high model accuracy and zero misclassification issues and relaxes distributional assumptions about sampling probabilities relative to other frequentist methods (Saltré et al., 2015). CRIWM inherits all those properties from GRIWM but substantially increases GRIWM's accuracy and precision and shows a lower sensitivity to sample size, dating errors and the frequency distribution of dated specimens in a fossil record. Frequentist methods are sometimes criticized for the width of the confidence intervals of estimated extinction times (Holdaway et al., 2014; Wang and Marshall, 2016), but such criticisms must be revisited by comparing CRIWM with Bayesian methods that, like CRIWM, control for the complex distributions inherent to ^{14}C errors.

The application of CRIWM and GRIWM often relies on the collation of chronometric data for a target taxon from multiple literature sources (see examples in Table S8). Therefore, users must always apply quality criteria to select reliable dates (Barnosky and Lindsey, 2010; Price et al., 2018; Rodríguez-Rey et al., 2015; Stuart, 2015), particularly when those observations consist of ^{14}C dates from skeletal materials (antler, bone, ivory, teeth) that are prone to contamination (Herrando-Pérez, 2021). Those criteria must be even more stringent for specimens dated towards the youngest and oldest ends of a time series as they will have the strongest effects on the calculation of extinction and arrival times, respectively. It should be born in mind that exchanges of carbon between a given fossil and the environment can make the ^{14}C date of the skeletal material in question younger or older than truth. The practicality is that the calibrated distribution of the date (re-sampled by CRIWM and Bayesian methods) will be misleading as it will be calculated from intervals of the calibration curve not representing the trend of ^{14}C decay experienced by the specimen (Supplementary Material SM1).

To estimate extinction time, frequentist methods, such as CRIWM and GRIWM, focus on a purely temporal axis of demographic variation. Future developments should map extinction and arrival time along geographical gradients (e.g., Bradshaw et al., 2021; Saltré et al., 2019; Wan and Zhang, 2017), which can be achieved by promoting dating efforts for species of interest and by combining specimens collected from the field and museum collections (Burgman et al., 1995). With the growing application of ^{14}C measurements to answer ecological and evolutionary questions (Marra, 2019; Swift et al., 2019; Taylor and Bar-Yosef, 2016), CRIWM should be useful to analyze a range of biological transitions, which are captured in ^{14}C chronologies, leading to the emergence and disappearance of populations and species, such as domestications (Fages et al., 2019; Frantz et al., 2016; Krajcarz et al., 2020), lineage replacements (Chang et al., 2017; Dehasque et al., 2021; Stanton et al., 2020) and human dispersal (Pettitt and Zilhão, 2015; Schmid et al., 2019; Waters et al., 2020).

Funding

The research was funded by an Australian Research Council Discovery Project (DP170104665). SHP supported by European Union's LIFE18 NAT/ES/000121 LIFE DIVAQUA, and FS supported by the Australian Research Council Centre of Excellence for Australian Biodiversity and Heritage Grant CE170100015 to Vera Weisbecker.

Author contributions

SHP conceived the idea, reviewed the literature, collected the mammal datasets, did the benchmarking and normality/multimodality analyses, and wrote the first draft of the manuscript and the package functions and the manuals. FS wrote the skeleton of the GRIWM function, formulated the unbiased estimator of extinction time, designed, ran, and interpreted the sensitivity analyses, and made the package publicly available on GitHub. Both contributed to manuscript revisions and approved submission.

Declaration of competing interest

The authors declare the following financial interests/personal relationships which may be considered as potential competing interests:

Salvador Herrando-Pérez reports financial support was provided by Australian Research Council. Frédérik Saltré reports financial support was provided by Australian Research Council. Salvador Herrando-Pérez reports financial support was provided by European Union (LIFE).

Data availability

The new *R* package *Rextinct* is freely available as an open-source *R* package and a user's manual under MIT licence at https://github.com/FredSaltre/CRIWM. Package features are described in Appendix A.

Acknowledgements

The research was funded by an Australian Research Council Discovery Project (DP170104665). SHP supported by European Union's LIFE18 NAT/ES/000121 LIFE DIVAQUA, and FS supported by the Australian Research Council Centre of Excellence for Australian Biodiversity and Heritage Grant CE170100015 to Vera Weisbecker. We thank Kieren J. Mitchell for his feedback on the final version of the manuscript, and George Perry, Matheus de Souza Lima Ribeiro, Paweł Mackiewicz, Natalia A. Villavicencio and Kurt M. Wilson for providing their datasets and faunal extinction estimates. Joël Chadoeuf provided statistical advice and commented an early version of this manuscript. SHP is grateful to Chris S. M. Turney and Alan Cooper for funding during the period of conception of the idea of this study, and to David R. Vieites for his unconditional support leading to this and other research papers in the last decade.

Appendix B. Supplementary data

Supplementary data to this article can be found online at https://doi.org/10.1016/j.quageo.2023.101489.

Appendix A. Package *Rextinct*

Rextinct is compatible with *R* versions from 3.6.3 (February 29, 2020) upwards on *Linux*, *Mac* and *Windows* operating systems. The package is freely available as an open-source *R* package and a user's manual under MIT licence at https://github.com/FredSaltre/CRIWM. It comprises three functions: *calendar*, *criwm* and *griwm*. Hereafter we explain the analytical steps run by each function, and benchmark their speed. The three functions load the input dataset (a text file without row names or column headings) from the working directory to the *R* environment through *data.table::fread* (Dowle and Srinivasan, 2019), which automatically detects file extension and column separators. Arguments and outputs per function are summarized in Tables 2 and 3.

A1. Functions criwm and griwm

These functions compute extinction time and have identical code structure with the following four analytical steps:

1. Data reading: the input data must contain two columns (column 1 = dates, column 2 = errors) and as many rows as dates in the time series. Users can specify which dates are ^{14}C, non-^{14}C, calibrated and non-calibrated using arguments in both functions (Table 2).
2. Calibration: calibration of non-calibrated ^{14}C dates is computed through *rcarbon::calibrate* (Crema and Bevan, 2021), and accepts the *IntCal20*, *IntCal13* and *NHPine16* calibration curves for Northern Hemisphere (Reimer et al., 2020), *SHCal20*, *SHCal13* and *SHKauri16* for Southern Hemisphere (Hogg et al., 2020) and *Marine20* and *Marine13* for marine (Heaton et al., 2020b) specimens. The *#20* series allows calibrations up to 55,000 calendar years BP, and the *#13* and *#16* series allow calibrations up to 50,000 calendar years BP. Post-bomb calibrations, after 1951 (Reimer et al., 2004), are not supported.
3. Re-sampling: function *griwm* re-samples from the normal distribution of each date in the time series (in calendar years) through *stats::rnorm* (R Core Team, 2020). Function *criwm* obtains the calibrated PDF from each non-calibrated ^{14}C date through *rcarbon::calibrate* (Crema and Bevan, 2021) and re-samples through *base::sample* (R Core Team, 2020) where re-sampling probabilities are weighted by the PDF of each date (Fig. 1). For time series combining a mix of chronometric techniques, function *criwm* re-samples non-^{14}C dates assuming normal errors and non-calibrated ^{14}C dates from their PDFs. If all dates in the time series are in calendar years, the calibration step is omitted, and function *criwm* re-samples normal errors from all dates and, only then, runs exactly like *griwm*.
4. Outputs: *criwm* and *griwm* return a list with three objects to the *R* console. The first object stores the argument values chosen by the user (Table 2), the second stores all dates (sorted from youngest to oldest) in years and their weighted averages (see below) in calendar years, and the third stores the extinction (or arrival) time (median with 95% inter-quantile rates for $\widehat{t_{\theta_F}}$ or $\widehat{t_{\theta_u}}$) in calendar years (Table 3). Users can save text files to the working directory including the second and third objects and the 10,000 re-sampled extinction times leading to $\widehat{t_{\theta_F}}$ or $\widehat{t_{\theta_u}}$ (Tables 2 and 3).

A2. Function calendar

This function calibrates ^{14}C dates from years to calendar years. It uses the same calibration curves as functions *criwm* and *griwm* (see above), with the following three analytical steps:

1. Data reading: The input data must comprise at least three columns. Columns 1 and 2 should contain the ^{14}C dates and their errors, respectively, and column 3 should contain the unique dating code given by a dating facility to each date, e.g., OxA-12345 represents the 12345th date produced by the Oxford Accelerator Unit (UK) (see examples in Fig. 1 footnote). The input data can include marine and terrestrial samples from different hemispheres, so an optional fourth column can be added up to the input file that contains the name of the specific calibration curve chosen to calibrate each ^{14}C date. When only one calibration curve is applied, this curve can be simply specified through one of the function's arguments (Table 2).
1. Calibration: function *calendar* emulates the calibration protocol of the field-standard software *oxcal* (Bronk Ramsey, 1995; Bronk Ramsey, 2017: https://c14.arch.ox.ac.uk/oxcal.html). It extracts the PDF of each non-calibrated ^{14}C date in F^{14}C (fraction modern Reimer et al., 2004) space (Heaton et al., 2020a) and normalizes it to a [0, 1] scale through *rcarbon::calibrate* (Crema and Bevan 2021).
2. Moments: *calendar* then computes (1) the four moments of the PDF (i.e., mean, variance, skewness, kurtosis), (2) the statistically supported modes defined as the highest posterior-probability-density regions falling in the shortest PDF intervals (see Hyndman, 1996) for confidence intervals of 1 and 2 standard deviations, and (3) three widely used point-estimates at which the non-calibrated ^{14}C date intercepts the calibration curve (Telford et al., 2004), namely the weighted average (mean of calibrated dates with non-zero probability weighted by their PDF probabilities), the median (calibrated date at which 50% of the PDF area is accounted for) and the mode (calibrated date at which the PDF probability is highest).
3. Outputs: the function returns a list with four objects to the *R* console. The first object stores the argument values chosen by the user (Table 2), the second stores the four PDF moments, the third stores the PDF modes, and the fourth stores the intercepts (average, median) with their respective confidence intervals. Optionally, users can save three text files to the working directory including the second to fourth objects (Tables 2 and 3).

A3. Benchmarking

In Supplementary Material SM7, we benchmarked computing time of the *Rextinct*'s three functions using 29 published GRIWM analysis on time series of (mega)fauna specimens, each including from 6 to 206 ^{14}C dates (Tables S8 and S9). We found that *griwm* and *criwm* completed computations in <1 and <8 min with (mega)fauna series of <60 ^{14}C dates (Table S10), and in <1 and <5 min with simulated series of <100 ^{14}C dates with a constant error of 50 years (Table S11), respectively. Function *calendar* calibrated all (mega)fauna series (Table S11) and up to 1000 simulated ^{14}C dates with a constant error of 50 years in <2 min (Table S12). The speed of the three functions decreased as the width of the errors of ^{14}C dates increased (Tables S11 and S12). Clearly, *griwm* is faster than *criwm* as re-sampling a complex PDF is slower than re-sampling a normal distribution, and the width of dating errors augments the computer resources allocated by *R* to re-sampling and calibration.

Table 2
Package *Rextinct* arguments for its three functions (*calendar*, *criwm*, *griwm*). Input data should be a text file, without row or column headings, including dated observations (rows) by dates (column 1) and errors (column 2), along with [only *calendar*] dating-lab identifier (column 3) and, optionally for non-calibrated ^{14}C dates, the name of the calibration curve to be used to calibrate each date (column 4). Saving options store text files of results in the working directory (see Table 3). CI = confidence interval (95% inter-quantile range), *P* = probability of a new observation younger (extinction) or older (arrival) than the youngest or oldest new observation respectively (formula 1), $\widehat{t_{\theta_\omega}}$ = 10,000 (default number) re-sampled extinction or arrival times (formula 2), $\widehat{t_{\theta_F}}$ = biased estimator of median extinction or arrival times (formula 2), $\widehat{t_{\theta_u}}$ = unbiased estimator of median extinction or arrival times (formula 3).

Function	Argument	Description
all	*chrono_data*	name of file containing the dated observations
criwm, *griwm*	*signor_lipps*	type of $\widehat{t_{\theta_F}}$ (extinction, arrival)
criwm, *griwm*	*biased*	type of estimator (biased, unbiased)
criwm, *griwm*	*alpha*	target probability (*P*)
criwm, *griwm*	*resample*	number of re-sampled time series
criwm, *griwm*	*radiocarbon*	row numbers including non-calibrated^{14}C dates
criwm, *griwm*	*calibra*	prompting calibration of non-calibrated^{14}C dates
all	*cal_curve*	calibration curve for non-calibrated^{14}C dates
all	*upper14C*	oldest calibrated date accepted
calendar	*cal_ci*	calibration CI (1 or 2 standard deviations)
all	*cal_save*	saving calibration outputs
criwm, *griwm*	*resample_save*	saving re-sampled $\widehat{t_{\theta_\omega}}$
criwm, *griwm*	*criwm_save*	saving CRIWM's $\widehat{t_{\theta_F}}$ [CI] or $\widehat{t_{\theta_u}}$ [CI]
criwm, *griwm*	*griwm_save*	saving GRIWM's $\widehat{t_{\theta_F}}$ [CI] or $\widehat{t_{\theta_u}}$ [CI]

Table 3
Package *Rextinct* outputs for its three functions (*calendar*, *criwm*, *griwm*). Storage space includes *R* for *R* environment or *T* for a text file saved in the working directory. Function arguments shown in Table 2. BP = Before Present, BCE = Before Current Era, BCY = Before Current Year, CI = confidence interval (95% inter-quantile range), PDF = Probability Density Function, $\widehat{t_{\theta_F}}$ (biased estimator) or $\widehat{t_{\theta_u}}$ (unbiased estimator) = median extinction or arrival times (formulas 2 and 3, respectively), $\widehat{t_{\theta_\omega}}$ = extinction time from each of 10,000 re-sampled time series.

Function	Description of outputs	Storage
calendar	arguments selected by user	*R*
	PDF moments (mean, variance, skewness, kurtosis)	*R*, *T*

(*continued on next page*)

Table 3 (*continued*)

Function	Description of outputs	Storage
	CI of statistically supported PDF modes	*R*, *T*
	non-calibrated and calibrated ^{14}C and non-^{14}C dates	*R*, *T*
criwm, *griwm*	arguments selected by user	*R*
	non-calibrated and calibrated ^{14}C and non-^{14}C dates	*R*, *T*
	$\widehat{t\theta_{tr}}$ [CI] or $\widehat{t\theta_{u}}$ [CI] in calendar years BP, BCE and BCY	*R*, *T*
	$\widehat{t\theta_{tr}}$ in calendar years BP	*T*

^{14}C calibrations.

References

Barnosky, A.D., Lindsey, E.L., 2010. Timing of Quaternary megafaunal extinction in South America in relation to human arrival and climate change. Quat. Int. 217, 10–29.

Boakes, E.H., Rout, T.M., Collen, B., 2015. Inferring species extinction: the use of sighting records. Methods Ecol. Evol. 6, 678–687.

Bradshaw, C.J.A., Cooper, A., Turney, C.S.M., Brook, B.W., 2012. Robust estimates of extinction time in the geological record. Quat. Sci. Rev. 33, 14–19.

Bradshaw, C.J.A., Norman, K., Ulm, S., Williams, A.N., Clarkson, C., Chadœuf, J., Lin, S. C., Jacobs, Z., Roberts, R.G., Bird, M.I., Weyrich, L.S., Haberle, S.G., O'Connor, S., Llamas, B., Cohen, T.J., Friedrich, T., Veth, P., Leavesley, M., Saltré, F., 2021. Stochastic models support rapid peopling of Late Pleistocene Sahul. Nat. Commun. 12, 2440.

Bronk Ramsey, C., 1995. Radiocarbon calibration and analysis of stratigraphy: the OxCal program. Radiocarbon 37, 425–430.

Bronk Ramsey, C., 2017. Methods for summarizing radiocarbon datasets. Radiocarbon 59, 1809–1833.

Burgman, M.A., Grimson, R.C., Ferson, S., 1995. Inferring threat from scientific collections. Conserv. Biol. 9, 923–928.

Chang, D., Knapp, M., Enk, J., Lippold, S., Kircher, M., Lister, A., MacPhee, R.D.E., Widga, C., Czechowski, P., Sommer, R., Hodges, E., Stümpel, N., Barnes, I., Dalén, L., Derevianko, A., Germonpré, M., Hillebrand-Voiculescu, A., Constantin, S., Kuznetsova, T., Mol, D., Rathgeber, T., Rosendahl, W., Tikhonov, A.N., Willerslev, E., Hannon, G., Lalueza-Fox, C., Joger, U., Poinar, H., Hofreiter, M., Shapiro, B., 2017. The evolutionary and phylogeographic history of woolly mammoths: a comprehensive mitogenomic analysis. Sci. Rep. 7, 44585.

Crema, E.R., Bevan, A., 2021. Inference from large sets of radiocarbon dates: software and methods. Radiocarbon 63, 23–39.

Da Veiga, S., 2015. Global sensitivity analysis with dependence measures. J. Stat. Comput. Simulat. 85, 1283–1305.

Dehasque, M., Pečnerová, P., Muller, H., Tikhonov, A., Nikolskiy, P., Tsigankova, V.I., Danilov, G.K., Díez-del-Molino, D., Vartanyan, S., Dalén, L., Lister, A.M., 2021. Combining Bayesian age models and genetics to investigate population dynamics and extinction of the last mammoths in northern Siberia. Quat. Sci. Rev. 259, 106913.

Dietl, G.P., Flessa, K.W., 2011. Conservation paleobiology: putting the dead to work. Trends Ecol. Evol. 26, 30–37.

Douglass, K., Hixon, S., Wright, H.T., Godfrey, L.R., Crowley, B.E., Manjakahery, B., Rasolondrainy, T., Crossland, Z., Radimilahy, C., 2019. A critical review of radiocarbon dates clarifies the human settlement of Madagascar. Quat. Sci. Rev. 221, 105878.

Dowle, M., Srinivasan, A., 2019. data.table: extension of 'data.frame'. https://CRAN.R-project.org/package=data.table (Version 1.12.8).

Elias, S.A., 2023. Late Pleistocene megafaunal extinctions. In: Elias, S.A., Mock, C.J. (Eds.), Encyclopedia of Quaternary Science. Elsevier, pp. 1–30.

Fages, A., Hanghøj, K., Khan, N., Gaunitz, C., Seguin-Orlando, A., Leonardi, M., McCrory Constantz, C., Gamba, C., Al-Rasheid, K.A.S., Albizuri, S., Alfarhan, A.H., Allentoft, M., Alquraishi, S., Anthony, D., Baimukhanov, N., Barrett, J.H., Bayarsaikhan, J., Benecke, N., Bernáldez-Sánchez, E., Berrocal-Rangel, L., Biglari, F., Boessenkool, S., Boldgiv, B., Brem, G., Brown, D., Burger, J., Crubézy, E., Daugnora, L., Davoudi, H., de Barros Damgaard, P., de los Ángeles de Chorro y de Villa-Ceballos, M., Deschler-Erb, S., Detry, C., Dill, N., do Mar Oom, M., Dohr, A., Ellingvåg, S., Erdenebaatar, D., Fathi, H., Felkel, S., Fernández-Rodríguez, C., García-Viñas, E., Germonpré, M., Granado, J.D., Hallsson, J.H., Hemmer, H., Hofreiter, M., Kasparov, A., Khasanov, M., Khazaeli, R., Kosintsev, P., Kristiansen, K., Kubatbek, T., Kuderna, L., Kuznetsov, P., Laleh, H., Leonard, J.A., Lhuillier, J., Liesau von Lettow-Vorbeck, C., Logvin, A., Lõugas, L., Ludwig, A., Luis, C., Arruda, A.M., Marques-Bonet, T., Matoso Silva, R., Merz, V., Mijiddorj, E., Miller, B.K., Monchalov, O., Mohaseb, F.A., Morales, A., Nieto-Espinet, A., Nistelberger, H., Onar, V., Pálsdóttir, A.H., Pitulko, V., Pitskhelauri, K., Pruvost, M., Rajic Sikanjic, P., Rapan Papeša, A., Roslyakova, N., Sardari, A., Sauer, E., Schafberg, R., Scheu, A., Schibler, J., Schlumbaum, A., Serrand, N., Serres-Armero, A., Shapiro, B., Sheikhi Seno, S., Shevnina, I., Shidrang, S., Southon, J., Star, B., Sykes, N., Taheri, K., Taylor, W., Teegen, W.-R., Trbojević Vukičević, T., Trixl, S., Tumen, D., Undrakhbold, S., Usmanova, E., Vahdati, A., Valenzuela-Lamas, S., Viegas, C., Wallner, B., Weinstock, J., Zaibert, V., Clavel, B., Lepetz, S., Mashkour, M., Helgason, A., Stefánsson, K., Barrey, E., Willerslev, E., Outram, A.K., Librado, P., Orlando, L., 2019. Tracking five millennia of horse management with extensive ancient genome time series. Cell 177, 1419–1435.

Feranec, R.S., Kozlowski, A.L., 2016. Implications of a Bayesian radiocarbon calibration of colonization ages for mammalian megafauna in glaciated New York State after the Last Glacial Maximum. Quat. Res. 85, 262–270.

Frantz, L.A.F., Mullin, V.E., Pionnier-Capitan, M., Lebrasseur, O., Ollivier, M., Perri, A., Linderholm, A., Mattiangeli, V., Teasdale, M.D., Dimopoulos, E.A., Tresset, A., Duffraisse, M., McCormick, F., Bartosiewicz, L., Gál, E., Nyerges, É.A., Sablin, M.V., Bréhard, S., Mashkour, M., Bălăşescu, A., Gillet, B., Hughes, S., Chassaing, O., Hitte, C., Vigne, J.-D., Dobney, K., Hänni, C., Bradley, D.G., Larson, G., 2016. Genomic and archaeological evidence suggest a dual origin of domestic dogs. Science 352, 1228–1231.

Frey, B.B., 2018. The SAGE Encyclopedia of Educational Research, Measurement, and Evaluation. SAGE Group, Thousand Oaks, California, UK.

García-León, M., 2018. Accelerator mass spectrometry (AMS) in radioecology. J. Environ. Radioact. 186, 116–123.

Gretton, A., Bousquet, O., Smola, A., Schölkopf, B., 2005. Measuring statistical dependence with Hilbert-Schmidt norms. In: Proceedings of the 16th International Conference on Algorithmic Learning Theory. Springer-Verlag, Singapore, pp. 63–77.

Hajdas, I., Ascough, P., Garnett, M.H., Fallon, S.J., Pearson, C.L., Quarta, G., Spalding, K. L., Yamaguchi, H., Yoneda, M., 2021. Radiocarbon dating. Nature Reviews Methods Primers 1, 62.

Heaton, T.J., Blaauw, M., Blackwell, P.G., Bronk Ramsey, C., Reimer, P.J., Scott, E.M., 2020a. The IntCal20 approach to radiocarbon calibration curve construction: a new methodology using Bayesian splines and errors-in-variables. Radiocarbon 62, 821–863.

Heaton, T.J., Köhler, P., Butzin, M., Bard, E., Reimer, R.W., Austin, W.E.N., Bronk Ramsey, C., Grootes, P.M., Hughen, K.A., Kromer, B., Reimer, P.J., Adkins, J., Burke, A., Cook, M.S., Olsen, J., Skinner, L.C., 2020b. Marine 20—the marine radiocarbon age calibration curve (0-55,000 cal BP). Radiocarbon 62, 779–820.

Herrando-Pérez, S., 2021. Bone need not remain an elephant in the room for radiocarbon dating. Royal Society Open Science 8, 201351.

Hogg, A.G., Heaton, T.J., Hua, Q., Palmer, J.G., Turney, C.S.M., Southon, J., Bayliss, A., Blackwell, P.G., Boswijk, G., Bronk Ramsey, C., Pearson, C., Petchey, F., Reimer, P., Reimer, R., Wacker, L., 2020. SHCal20 Southern Hemisphere calibration, 0-55,000 years cal BP. Radiocarbon 62, 759–778.

Holdaway, R.N., Allentoft, M.E., Jacomb, C., Oskam, C.L., Beavan, N.R., Bunce, M., 2014. An extremely low-density human population exterminated New Zealand moa. Nat. Commun. 5, 5436.

Hughen, K., Lehman, S., Southon, J., Overpeck, J., Marchal, O., Herring, C., Turnbull, J., 2004. ^{14}C activity and global carbon cycle changes over the past 50,000 years. Science 303, 202–207.

Hyndman, R.J., 1996. Computing and graphing highest density regions. Am. Statistician 50, 120–126.

Iooss, B., Da Veiga, S., Janon, A., Pujol, G., 2021. Sensitivity: global sensitivity analysis of model outputs, (version 1.27.0). https://cran.r-project.org/web/packages/sensitivity.

Keenan, D.J., 2012. Calibration of a radiocarbon age. Nonlinear Process Geophys. 19, 345–350.

Kouvari, M., van der Geer, A.A.E., 2018. Biogeography of extinction: the demise of insular mammals from the Late Pleistocene till today. Palaeogeogr. Palaeoclimatol. Palaeoecol. 505, 295–304.

Krajcarz, M., Krajcarz, M.T., Baca, M., Baumann, C., Van Neer, W., Popović, D., Sudoł-Procyk, M., Wach, B., Wilczyński, J., Wojenka, M., Bocherens, H., 2020. Ancestors of domestic cats in Neolithic Central Europe: isotopic evidence of a synanthropic diet. Proc. Natl. Acad. Sci. USA 117, 17710–17719.

Lindgren, B., 2017. Statistical Theory, fourth ed. Routledge, UK.

Lister, A.M., Stuart, A.J., 2019. The extinction of the giant deer *Megaloceros giganteus* (Blumenbach): new radiocarbon evidence. Quat. Int. 500, 185–203.

Marra, J.F., 2019. Hot carbon: carbon-14 and a revolution in science. Columbia University Press, New York, USA.

McInerny, G.J., Roberts, D.L., Davy, A.J., Cribb, P.J., 2006. Significance of sighting rate in inferring extinction and threat. Conserv. Biol. 20, 562–567.

McKay, M.D., Beckman, R.J., Conover, W.J., 1979. Comparison of three methods for selecting values of input variables in the analysis of output from a computer code. Technometrics 21, 239–245.

Mitchell, K.J., Rawlence, N.J., 2021. Examining natural history through the lens of palaeogenomics. Trends Ecol. Evol. 36, 258–267.

Nogués-Bravo, D., Rodríguez, J., Hortal, J., Batra, P., Araújo, M.B., 2008. Climate change, humans, and the extinction of the woolly mammoth. PLoS Biol. 6, e79.

Olsson, I.U., 1989. The ^{14}C method — its possibilities and some pitfalls. PACT Publications 24, 161–177.

Pavón-Carrasco, F.J., Gómez-Paccard, M., Campuzano, S.A., González-Rouco, J.F., Osete, M.L., 2018. Multi-centennial fluctuations of radionuclide production rates are modulated by the Earth's magnetic field. Sci. Rep. 8, 9820.
Perez, S.I., Postillone, M.B., Rindel, D., Gobbo, D., Gonzalez, P.N., Bernal, V., 2016. Peopling time, spatial occupation and demography of Late Pleistocene–Holocene human population from Patagonia. Quat. Int. 425, 214–223.
Pettitt, P., Zilhão, J., 2015. Problematizing Bayesian approaches to prehistoric chronologies. World Archaeol. 47, 525–542.
Politis, G.G., Messineo, P.G., Stafford, T.W., Lindsey, E.L., 2019. Campo Laborde: a Late Pleistocene giant ground sloth kill and butchering site in the Pampas. Sci. Adv. 5, eaau4546.
Price, G.J., Louys, J., Faith, J.T., Lorenzen, E., Westaway, M.C., 2018. Big data little help in megafauna mysteries. Nature 558, 23–25.
Pugach, I., Hübner, A., Hung, H.-c., Meyer, M., Carson, M.T., Stoneking, M., 2021. Ancient DNA from Guam and the peopling of the pacific. Proc. Natl. Acad. Sci. USA 118, e2022112118.
R Core Team, 2020. R: a language and environment for statistical computing. R Foundation for Statistical Computing, Vienna, Austria.
Raup, D.M., 1986. Biological extinction in earth history. Science 231, 1528–1533.
Raup, D.M., 1994. The role of extinction in evolution. Proc. Natl. Acad. Sci. USA 91, 6758–6763.
Reimer, P.J., Austin, W.E.N., Bard, E., Bayliss, A., Blackwell, P.G., Bronk Ramsey, C., Butzin, M., Cheng, H., Edwards, R.L., Friedrich, M., Grootes, P.M., Guilderson, T.P., Hajdas, I., Heaton, T.J., Hogg, A.G., Hughen, K.A., Kromer, B., Manning, S.W., Muscheler, R., Palmer, J.G., Pearson, C., van der Plicht, J., Reimer, R.W., Richards, D.A., Scott, E.M., Southon, J.R., Turney, C.S.M., Wacker, L., Adolphi, F., Büntgen, U., Capano, M., Fahrni, S.M., Fogtmann-Schulz, A., Friedrich, R., Köhler, P., Kudsk, S., Miyake, F., Olsen, J., Reinig, F., Sakamoto, M., Sookdeo, A., Talamo, S., 2020. The IntCal20 Northern Hemisphere radiocarbon age calibration curve (0-55 cal kBP). Radiocarbon 62, 725–757.
Reimer, P.J., Brown, T.A., Reimer, R.W., 2004. Discussion: reporting and calibration of post-bomb ^{14}C data. Radiocarbon 46, 1299–1304.
Rivadeneira, M.M., Hunt, G., Roy, K., 2009. The use of sighting records to infer species extinctions: an evaluation of different methods. Ecology 90, 1291–1300.
Rodríguez-Rey, M., Herrando-Pérez, S., Gillespie, R., Jacobs, Z., Saltré, F., Brook, B.W., Prideaux, G.J., Roberts, R.G., Cooper, A., Alroy, J., Miller, G.H., Bird, M.I., Johnson, C.N., Beeton, N., Turney, C.S.M., Bradshaw, C.J.A., 2015. Criteria for assessing the quality of Middle Pleistocene to Holocene vertebrate fossil ages. Quat. Geochronol. 30, 69–79.
Roth, R., Joos, F., 2013. A reconstruction of radiocarbon production and total solar irradiance from the Holocene ^{14}C and CO_2 records: implications of data and model uncertainties. Clim. Past 9, 1879–1909.
Saltelli, A., Ratto, M., Andres, T., Campolongo, F., Cariboni, J., Gatelli, D., Saisana, M., Tarantola, S., 2007. Global Sensitivity Analysis. The Primer. John Wiley & Sons, Ltd., The Atrium, West Sussex, England, UK.
Saltré, F., Brook, B.W., Rodríguez-Rey, M., Cooper, A., Johnson, C.N., Turney, C.S.M., Bradshaw, C.J.A., 2015. Uncertainties in dating constrain model choice for inferring extinction time from fossil records. Quat. Sci. Rev. 112, 128–137.
Saltré, F., Chadoeuf, J., Peters, K.J., McDowell, M.C., Friedrich, T., Timmermann, A., Ulm, S., Bradshaw, C.J.A., 2019. Climate-human interaction associated with southeast Australian megafauna extinction patterns. Nat. Commun. 10, 5311.
Saltré, F., Rodríguez-Rey, M., Brook, B.W., Johnson, C.N., Turney, C.S.M., Alroy, J., Cooper, A., Beeton, N., Bird, M.I., Fordham, D.A., Gillespie, R., Herrando-Pérez, S., Jacobs, Z., Miller, G.H., Nogués-Bravo, D., Prideaux, G.J., Roberts, R.G., Bradshaw, C.J.A., 2016. Climate change not to blame for late Quaternary megafauna extinctions in Australia. Nat. Commun. 7, 10511.
Schmid, M.M.E., Wood, R., Newton, A.J., Vésteinsson, O., Dugmore, A.J., 2019. Enhancing radiocarbon chronologies of colonization: chronometric hygiene revisited. Radiocarbon 61, 629–647.
Signor III, P.W., Lipps, J.H., 1982. Sampling bias, gradual extinction patterns and catastrophes in the fossil record. In: Silver, L.T., Schultz, P.H. (Eds.), Geological implications of impacts of large asteroids and comets on the Earth. Geological Society of America, pp. 291–296.
Solow, A.R., 2005. Inferring extinction from a sighting record. Math. Biosci. 195, 47–55.
Solow, A.R., Roberts, D.L., Robbirt, K.M., 2006. On the Pleistocene extinctions of Alaskan mammoths and horses. Proc. Natl. Acad. Sci. USA 103, 7351–7353.
Stanton, D.W.G., Alberti, F., Plotnikov, V., Androsov, S., Grigoriev, S., Fedorov, S., Kosintsev, P., Nagel, D., Vartanyan, S., Barnes, I., Barnett, R., Ersmark, E., Döppes, D., Germonpré, M., Hofreiter, M., Rosendahl, W., Skoglund, P., Dalén, L., 2020. Early Pleistocene origin and extensive intra-species diversity of the extinct cave lion. Sci. Rep. 10, 12621.
Stuart, A.J., 2015. Late Quaternary megafaunal extinctions on the continents: a short review. Geol. J. 50, 338–363.
Stuart, A.J., Sulerzhitsky, L.D., Orlova, L.A., Kuzmin, Y.V., Lister, A.M., 2002. The latest woolly mammoths (*Mammuthus primigenius* Blumenbach) in Europe and Asia: a review of the current evidence. Quat. Sci. Rev. 21, 1559–1569.
Swift, J.A., Bunce, M., Dortch, J., Douglass, K., Faith, J.T., Fellows Yates, J.A., Field, J., Haberle, S.G., Jacob, E., Johnson, C.N., Lindsey, E., Lorenzen, E.D., Louys, J., Miller, G., Mychajliw, A.M., Slon, V., Villavicencio, N.A., Waters, M.R., Welker, F., Wood, R., Petraglia, M., Boivin, N., Roberts, P., 2019. Micro methods for megafauna: novel approaches to Late Quaternary extinctions and their contributions to faunal conservation in the Anthropocene. Bioscience 69, 877–887.
Taylor, R.E., Bar-Yosef, O., 2016. Radiocarbon dating. An archaeological perspective. Routhledge, New York, USA.
Telford, R.J., Heegaard, E., Birks, H.J.B., 2004. The intercept is a poor estimate of a calibrated radiocarbon age. Holocene 14, 296–298.
van der Plicht, J., Palstra, S.W.L., 2016. Radiocarbon and mammoth bones: what's in a date. Quat. Int. 406, 246–251.
Wan, X., Zhang, Z., 2017. Climate warming and humans played different roles in triggering Late Quaternary extinctions in east and west Eurasia. Proceedings of the Royal Society B 284, 20162438.
Wang, S.C., Marshall, C.R., 2016. Estimating times of extinction in the fossil record. Biol. Lett. 12, 20150989.
Waters, M.R., Stafford, T.W., Carlson, D.L., 2020. The age of Clovis—13,050 to 12,750 cal yr B.P. Sci. Adv. 6, eaaz0455.
White, L.C., Saltré, F., Bradshaw, C.J.A., Austin, J.J., 2018. High-quality fossil dates support a synchronous, Late Holocene extinction of devils and thylacines in mainland Australia. Biol. Lett. 14, 20170642.